

Development of $\langle 110 \rangle$ texture in copper thin films

H. L. Wei

*Department of Mechanical Engineering, Hong Kong Polytechnic University, Hong Kong
and Department of Physics, Huazhong University of Science and Technology, Wuhan, 430074 China*

Hanchen Huang^{a)} and C. H. Woo

Department of Mechanical Engineering, Hong Kong Polytechnic University, Hong Kong

R. K. Zheng, G. H. Wen, and X. X. Zhang

Department of Physics and Institute of Nano Science and Technology, Hong Kong University of Science and Technology, Hong Kong

(Received 30 November 2001; accepted for publication 1 February 2002)

Apart from the scientific interest, texture development in copper thin films is of crucial importance to their applications as interconnects or corrosion resistant coating. We report here a dominant $\langle 110 \rangle$ texture of copper thin films—preferred for oxidation-resistant applications—deposited by direct current magnetron sputtering. Scanning electron microscopy shows that the copper films go through a transition from $\langle 111 \rangle$ columns to $\langle 110 \rangle$ hillocks as the deposition proceeds. Cross-sectional transmission electron microscopy (TEM) indicates that the $\langle 110 \rangle$ grains nucleate at boundaries of $\langle 111 \rangle$ grains. Further, we have proposed a stress-driven nucleation and growth model of $\langle 110 \rangle$ grains based on the x-ray diffraction characterization and the TEM observations. © 2002 American Institute of Physics. [DOI: 10.1063/1.1466518]

As the dimension of integrated circuits continues to shrink, it is becoming ever more crucial to control the microstructure—in particular, the texture—of metal thin films as interconnects. Tremendous amounts of effort has been devoted to texture optimization of aluminum interconnects.^{1–3} With increasing use of copper in place of aluminum as interconnects, development of the $\langle 111 \rangle$ texture in copper has been a focus in recent investigations.^{4–6} On the other hand, development of the $\langle 110 \rangle$ texture is also preferred in oxidation-resistant applications.^{7,8} As a result, numerous investigations have focused on these two textures, $\langle 111 \rangle$ and $\langle 110 \rangle$, in copper thin films.

These two textures, $\langle 111 \rangle$ and $\langle 110 \rangle$, have been observed in copper films deposited by electroplating,^{9,10} cathodic vacuum arcing,¹¹ and dry etching.¹² The magnetron sputtering deposition—an economic approach in manufacturing—has been found to produce copper films of only weak $\langle 110 \rangle$ texture.¹³ For face-center-cubic metals, it has been demonstrated^{11,14} that incident energetic particles favor the development of $\langle 110 \rangle$ over the $\langle 111 \rangle$ texture, due to the easier channeling, and thereby less localized radiation damage in the $\langle 110 \rangle$ grains. When the energy of incident particles is in the range of tens of electron volts, channeling effects are absent, and the heat deposition from the kinetic energy favors the thermodynamically preferred $\langle 111 \rangle$ texture.

Apart from the damage effects, it is known that stress may be produced in thin films by energetic particles.^{11,15} Further, annealing experiments show that stress may favor the $\langle 110 \rangle$ texture in copper films.¹⁶ Under stress and at high temperature, hillocks of $\langle 110 \rangle$ texture grow at the expense of grains of $\langle 111 \rangle$ texture.^{17,18} It is scientifically interesting and

technologically important to investigate whether the $\langle 110 \rangle$ hillocks are also formed during deposition.

In this letter, we report the development of a strong $\langle 110 \rangle$ texture in copper thin films, during direct current (dc) magnetron sputtering deposition. The experimental conditions are briefly summarized as follows. The sputtering power is variable from 50 to 200 W, and the chamber is filled with 99.999% Ar, flowing into the chamber at a rate of 8 sccm. During the deposition, the base pressure is about 5.0×10^{-8} Torr and the working pressure is about 2.5×10^{-3} Torr. The target is a block of 99.997% copper, and is sputter cleaned in Ar gas for 10 min before deposition. The substrate, which is 5 cm away from the target, is an n-type Si(111) wafer of resistivity 10–12 Ω cm. It can either be used as a clean Si substrate or oxidized before deposition—effectively making a SiO₂ substrate. In the latter case, SiO₂ layers of about 0.1 μ m are the result of annealing at 300 °C in air for 1 h. In all cases, the substrate is cleaned ultrasonically in alcohol and then acetone. The copper films are usually about 0.7 μ m in thickness. For the four different sputtering powers of 50, 100, 150, and 200 W, the deposition rates are found to be 28, 48, 62, and 75 nm/min, respectively, and the substrate temperature is maintained at $0.22T_m$. The films are characterized using x-ray diffraction (XRD), scanning electron microscopy (SEM), and transmission electron microscopy (TEM).

As shown in Fig. 1(a), the copper film is uniform and columnar when the deposition power is 50 W. When the deposition power is kept at 100 W, the film is initially uniform and subsequently develops into hillocks, as shown in Fig. 1(b). At the power of 50 W, hillocks never form. However, at 100 or 150, or 200 W, the hillocks start to develop when the film is about 0.2–0.3 μ m thick. To identify the textures of films deposited at various sputtering powers, we have measured the XRD intensity for each of the films. As

^{a)}Author to whom correspondence should be addressed; electronic mail: Hanchen.Huang@polyu.edu.hk and hanchen@rpi.edu after summer 2002.

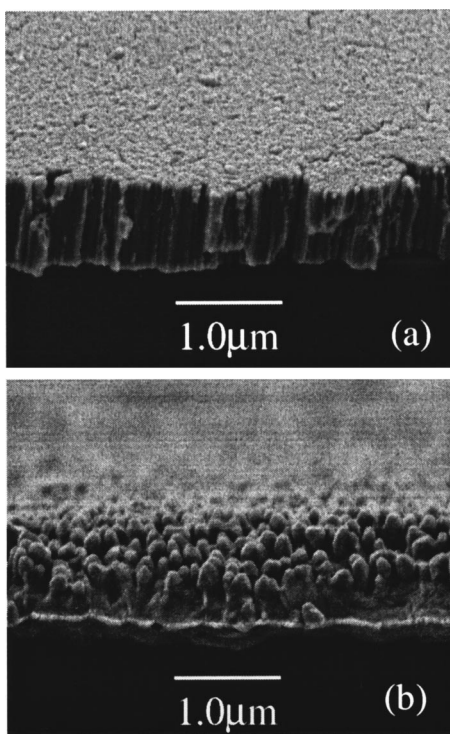


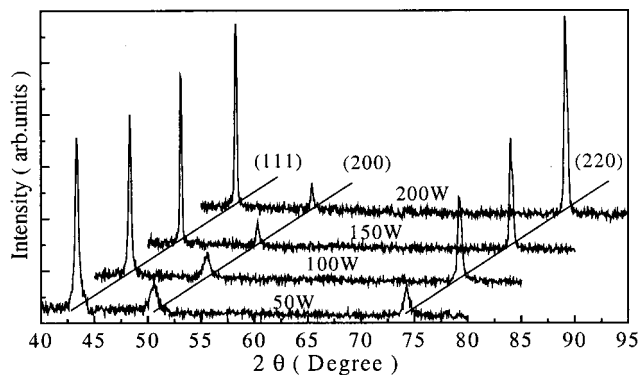
FIG. 1. Cross-sectional SEM of copper films deposited on a SiO₂/Si(111) wafer at (a) 50 W and (b) 100 W.

shown in Fig. 2, the intensity of the $\langle 110 \rangle$ peak [or (220) in XRD terminology] increases with increasing sputtering power. This observation applies to both substrates, Si(111) and SiO₂, although the $\langle 110 \rangle$ dominance is not as strong in the case of the Si(111) substrate.

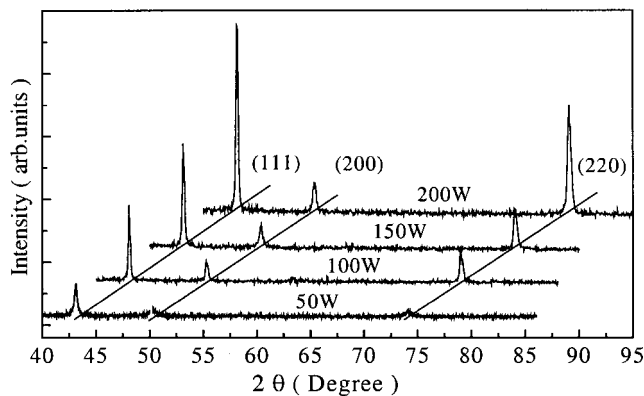
Variation of XRD intensity is a direct result of microstructure evolution in the film. A horizontal cross section in the middle of the copper film deposited at 100 W is examined using TEM. In Fig. 3, grain α in the center has a $\langle 110 \rangle$ orientation—as shown by the convergent electron-beam diffraction (inset of Fig. 3)—the diffraction pattern shows that the grain at the upper-left corner and that at the lower left corner are also $\langle 110 \rangle$. According to Figs. 1 and 2, the $\langle 110 \rangle$ grains consist of primarily hillocks, which are in the shape of cones. Indeed, this is shown by the thickness contours on the sides of the $\langle 110 \rangle$ grains in Fig. 3.

These cone-shaped $\langle 110 \rangle$ grains must have either grown from pre-existing small grains, or nucleated during the deposition. Figure 4(a) shows a hillock surrounded by a few grains. There are three grains near the bottom of the hillock. It is not impossible that the hillock is an extension of a grain in front of or behind the paper. However, the cone shape of the hillocks in Figs. 1 and 3 does support that the hillock nucleates near boundaries or the triple junction of these three surrounding grains.

Accepting that the $\langle 110 \rangle$ hillocks have nucleated from exiting interfaces, the next question is, what is the driving force? According to XRD measurements carried out before hillock formation, spacing of the (111) planes of the $\langle 111 \rangle$ grains is increased to 0.2088, 0.2097, 0.2098, and 0.2098 nm for sputtering powers of 50, 100, 150, and 200 W, respectively. Using a Young's modulus of 130 GPa, we may estimate the stress in $\langle 111 \rangle$ grains to be more than 600 MPa when the power is higher than 100 W. The disparity of elastic



(a)



(b)

FIG. 2. XRD intensity copper films deposited on (a) a SiO₂/Si(111) wafer and (b) a Si(111) wafer at various sputtering powers.

strain energies in $\langle 110 \rangle$ and $\langle 111 \rangle$ grains—due to elastic anisotropy—is probably the driving force for the nucleation of the $\langle 110 \rangle$ grains. Based on the stress analysis and the TEM/XRD observations, it seems logical to conclude that the $\langle 110 \rangle$ grains nucleate at boundaries of $\langle 111 \rangle$ grains during

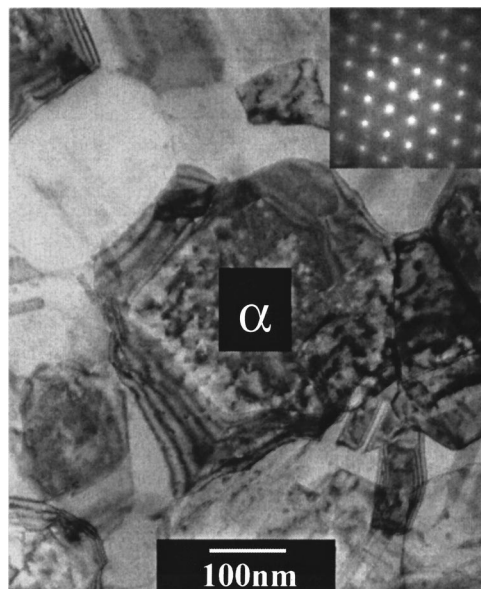
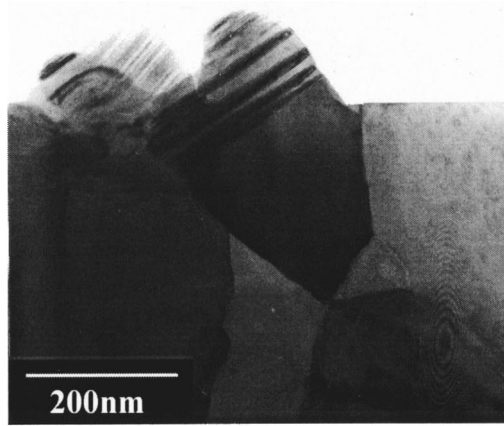
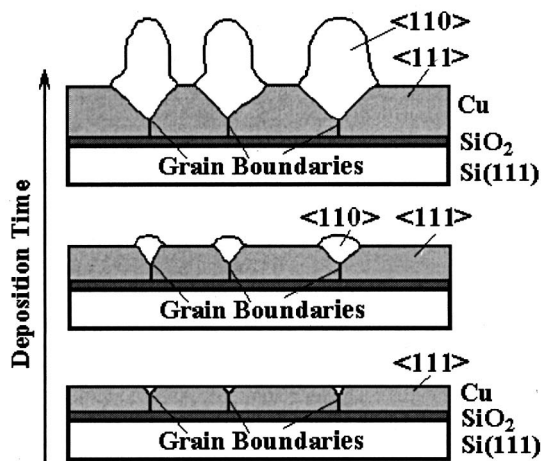


FIG. 3. Bright-field TEM of copper film deposited on a SiO₂/Si(111) wafer at 100 W. A typical $\langle 110 \rangle$ grain is marked as “ α .” Inset is the convergent electron-beam diffraction of the grain “ α .”



(a)



(b)

FIG. 4. (a) Bright-field TEM of a vertical cross section of the copper film deposited on a $\text{SiO}_2/\text{Si}(111)$ wafer at 100 W, when a hillock has just formed. (b) Schematic of our proposed model of nucleation and growth of the $\langle 110 \rangle$ grains (white) from boundaries or triple junctions of $\langle 111 \rangle$ grains (gray).

deposition, due to stresses developed during the deposition. This idea is schematically demonstrated in Fig. 4(b). Nucleation of the $\langle 110 \rangle$ grains is a combination of stochastic fluctuation and elastic anisotropy, and the growth is mainly dictated by the elastic anisotropy. These elastic energy effects have also been considered in annealing experiments.^{17,18}

In summary, we have deposited copper films with strong $\langle 110 \rangle$ texture—either comparable to or stronger than the

$\langle 111 \rangle$ texture. The microstructure characterizations indicate that a film of uniform $\langle 111 \rangle$ texture first forms, followed by the formation of $\langle 110 \rangle$ hillocks at boundaries of $\langle 111 \rangle$ grains; the $\langle 110 \rangle$ grains grow larger as the film becomes thicker. The stress in the film is found to be on the order of 600 MPa. We propose that $\langle 110 \rangle$ grains nucleate at boundaries or triple junctions of $\langle 111 \rangle$ grains due to disparity of elastic strain energy—caused by elastic anisotropy—in $\langle 110 \rangle$ and $\langle 111 \rangle$ grains. Although the proposed model in this letter is primitive, it does account for the experimental observations. Molecular dynamics simulations are underway to validate this proposal.

The work described in this letter was supported by grants from the Research Grants Council of the Hong Kong Special Administrative Region (PolyU 1/99C, PolyU 5146/99E, PolyU 5152/00E, PolyU 5161/01E, and HKUST 6165/01P).

¹D. B. Knorr and T.-M. Lu, Appl. Phys. Lett. **54**, 2210 (1989).

²H. Onoda, M. Kageyama, and K. Hashimoto, J. Appl. Phys. **77**, 885 (1995).

³H. Huang, G. H. Gilmer, and T. Diaz de la Rubia, J. Appl. Phys. **84**, 3636 (1998); G. H. Gilmer, H. Huang, T. Diaz de la Rubia, J. D. Torre, and F. Baumann, Thin Solid Films **365**, 189 (2000); H. Huang and G. H. Gilmer, J. Comput.-Aided Mater. Des. **7**, 203 (2001).

⁴J. L. Hurd, K. P. Rodbell, L. M. Gignac, L. A. Clevenger, R. C. Iggulden, R. F. Schnabel, S. J. Weber, and N. H. Schmidt, Appl. Phys. Lett. **72**, 326 (1998).

⁵D. P. Tracy, D. B. Knorr, and K. P. Rodbell, J. Appl. Phys. **76**, 2671 (1994).

⁶J. A. Nucci, R. R. Keller, J. E. Sanchez, Jr., and Y. S. Diamond, Appl. Phys. Lett. **69**, 4017 (1996).

⁷F. W. Young, Jr., J. V. Cathcart, and A. T. Gwathmey, Acta Metall. **4**, 145 (1956).

⁸J. Li, J. W. Mayer, and E. G. Colgan, J. Appl. Phys. **70**, 2820 (1991).

⁹L. Lu, N. R. Tao, L. B. Wang, B. Z. Ding, and K. Lu, J. Appl. Phys. **89**, 6408 (2001).

¹⁰C. H. Seah, S. Mridha, and L. H. Chan, J. Vac. Sci. Technol. B **17**, 2352 (1999).

¹¹Y. H. Cheng, B. K. Tay, S. P. Lau, X. Shi, and H. S. Tan, J. Vac. Sci. Technol. B **19**, 2102 (2001).

¹²W. Lee, H. Yang, P. J. Reucroft, H. Soh, J. Kim, S. Woo, and J. Lee, Thin Solid Films **392**, 122 (2001).

¹³D. P. Tracy and D. B. Knorr, J. Electron. Mater. **22**, 611 (1993).

¹⁴L. Dong, D. J. Srolovitz, G. S. Was, Q. Zhao, and A. D. Rllett, J. Mater. Res. **16**, 210 (2001); L. Dong and D. J. Srolovitz, Appl. Phys. Lett. **75**, 584 (1999).

¹⁵P. Ziemann and E. Kay, J. Vac. Sci. Technol. A **1**, 512 (1983).

¹⁶J. M. Zhang, K. W. Xu, and J. W. He, J. Mater. Sci. Lett. **18**, 471 (1999); J. Cryst. Growth **226**, 168 (2001).

¹⁷J. E. Sanchez, Jr., and A. Artz, Scr. Metall. Mater. **27**, 285 (1992).

¹⁸A. Gladkikh, Y. Lereah, E. Glickman, and M. Karpovski, Appl. Phys. Lett. **66**, 1214 (1995).